Comparing bias correction methods in downscaling meteorological variables for hydrologic impact study in an arid area in China

G.H. Fang [1, 2, 3], J. Yang [1*,4], Y.N. Chen [1], C. Zammit [4]

[1] State Key Laboratory of Desert and Oasis Ecology, Xinjiang Institute of Ecology and Geography, Chinese Academy of Sciences, Xinjiang, China

[2] University of Chinese Academy of Sciences, Beijing, China

[3] Department of Geography, Ghent University, Ghent, Belgium

[4] National Institute of Water and Atmospheric Research, Christchurch, New Zealand

Corresponding author:

Jing Yang*

State Key Laboratory of Desert and Oasis Ecology, Xinjiang Institute of Ecology and Geography, Chinese Academy of Sciences, Xinjiang, 830011, China

818 South Beijing Road, Urumqi, Xinjiang, 830011, China

Tel: +86-991-7823171

Email: yangjing@ms.xjb.ac.cn

Comparing bias correction methods in downscaling meteorological variables for hydrologic impact study in an arid area in China

Abstract:

Water resources are essential to the ecosystem and social economy in the desert and oasis of the arid Tarim River Basin, Northwest China, and expected to be vulnerable to climate change. It has been demonstrated that Regional Climate Models (RCM) provide more reliable results for regional impact study of climate change (e.g., on water resources) than General Circulation Models (GCM). However, due to their considerable bias it is still necessary to apply bias correction before they are used for water resources research. In this paper, after a sensitivity analysis on input meteorological variables based on Sobol' method, we compared five precipitation correction methods and three temperature correction methods in downscaling RCM simulations applied over the Kaidu River Basin, one of the headwaters of the Tarim River Basin. Precipitation correction methods applied include Linear Scaling (LS), LOCal Intensity scaling (LOCI), Power Transformation (PT), Distribution Mapping (DM) and Quantile Mapping (QM); while temperature correction methods are LS, VARIance scaling (VARI) and DM. The corrected precipitation and temperature were compared to the observed meteorological data, prior to be used as meteorological inputs of a distributed hydrologic model to study their impacts on streamflow. The results show: 1) Streamflows are sensitive to precipitation, temperature, solar radiation but not to relative humidity and wind speed; 2) Raw RCM simulations are heavily

biased from observed meteorological data, and its use for streamflow simulations results in large biases from observed streamflow, and all bias correction methods effectively improved these simulations; 3) For precipitation, PT and QM methods performed equally best in correcting the frequency-based indices (e.g., standard deviation, percentile values) while LOCI method performed best in terms of the time-series based indices (e.g., Nash-Sutcliffe coefficient, R^2); 4) For temperature, all correction methods performed equally well in correcting raw temperature; 5) For simulated streamflow, precipitation correction methods have more significant influence than temperature correction methods and the performances of streamflow simulations are consistent with those of corrected precipitation, i.e., PT and QM methods performed equally best in correcting flow duration curve and peak flow while LOCI method performed best in terms of the time-series based indices. The case study is for an arid area in China based on a specific RCM and hydrologic model, but the methodology and some results can be applied to other areas and models.

1. Introduction

In recent decades, the ecological situation of the Tarim River Basin in China has seriously degraded especially in the lower reaches of the Tarim River due to water scarcity. In the meantime, climate change is significant in this region with an increase in temperature at a rate of 0.33 ~ 0.39 ℃/decade and a slight increase in precipitation (Li et al., 2012) over the past 5 decades. Under the context of regional climate change, water resources in this region are expected to be more unstable and ecosystems are likely to suffer from severe water stress because the hydrologic system of the arid region is particularly vulnerable to climate change (Arnell et al., 1992; Shen and Chen, 2010; Wang et al., 2013). The impact of climate change on hydrologic system has already been observed and it is expected that the hydrological system will continue to change in the future (Liu et al., 2010, 2011; Chen et al., 2010). Therefore, projecting reliable climate change and its impact on hydrology are important to study the ecology in the Tarim River Basin.

Only recently efforts have been made to evaluate and project the impact of climate change on hydrology in the Tarim River Basin. These studies include research on the relationships of meteorological variables and streamflow based on the historical measurements (e.g. Chen et al., 2013c; Xu et al., 2013), and use of the GCM outputs to drive a hydrologic model to study potential climate change on water resources (Liu et al., 2010, 2011). Study of historical climate - hydrology relationships has limited applications on future water resources management, especially under the context of global climate change. Though GCMs have been widely used to study impacts of

future climate change on hydrological systems and water resources, they are impeded by their inability to provide reliable information at the hydrological scales (Maraun et al., 2010; Giorgi, 1990). In particular, for mountainous regions, fine scale information such as the altitude-dependent precipitation and temperature information, which is critical for hydrologic modeling, is not represented in GCMs (Seager and Vecchi, 2010). Therefore, recent studies tend to use the higher-resolution Regional Climate Models (RCMs) to preserve the physical coherence between atmospheric and land surface variables (Bergstrom et al., 2001; Anderson et al., 2011). As such, when evaluating the impact of climate change on water resources on a watershed scale, the use of RCMs instead of GCMs is preferable since RCMs have been proved to provide more reliable results for impact study of climate change on regional water resources than GCM models (Buytaert et al., 2010; Elguindi et al., 2011). However, the raw RCM simulations may be still biased especially in the mountainous regions (Murphy, 1999; Fowler et al., 2007), which makes the use of RCM outputs as direct input for hydrological model challenging. As a result it is of significance to properly correct the RCM simulated meteorological variables before they are used to drive a hydrological model especially in an arid region where the hydrology is sensitive to climate changes.

Several bias correction methods have been developed to downscale meteorological variables from the RCMs, ranging from the simple scaling approach to sophisticated distribution mapping (Teutschbein and Seibert, 2012). And their applicability in the arid Tarim River Basin has not been investigated, thereby, evaluating and finding the appropriate bias correction method is necessary to evaluate the impact of climate

84 change on water resources.

85 This study evaluates performances of five precipitation bias correction methods
86 and three temperature bias correction methods in downscaling RCM simulations and
87 applied to the Kaidu River Basin, one of the most important headwaters of the Tarim
88 River. These bias correction methods include most frequently used bias correction
89 methods. We compare their performances in downscaling precipitation and temperature
90 and evaluate their impact on streamflow through hydrological modeling.

91 The paper is constructed as follows: Section 2 introduces the study area and
92 data; Section 3 describes the bias correction methods for precipitation and temperature
93 along with the hydrological model, sensitivity analysis method and result analysis
94 strategy; and then Section 4 presents results and discussion, followed by conclusions in
95 Section 5.

96

97

98 **2 Study area and data**

99 2.1 Study area and observed data

100 The Kaidu River Basin, with a drainage area of 18,634 km^2 above the Dashankou
101 hydrological station, is located on the south slope of the Tianshan Mountains in
102 Northwest China (Fig. 1). Its altitude ranges from 1,342 m to 4,796 m above sea level
103 (a.s.l.) with an average elevation of 2,995 m, and its climate is temperate continental
104 with alpine climate characteristics. As one of the headwaters of the Tarim River, it

105 provides water resources for agricultural activity and ecological environment of the
106 oasis in the lower reaches. This oasis, with a population of over 1.15 million, is
107 stressed by lack of water and water resources are the main factor constricting the
108 development (Chen et al., 2013b). Therefore, projecting the impact of future climate
109 change on water resources is urgent to the sustainable development of this region.

110 Daily observed meteorological data, including precipitation, maximum/minimum
111 temperature, wind speed and relative humidity of two meteorological stations
112 (Bayanbulak and Baluntai, stars in Fig. 1), are from the China Meteorological Data
113 Sharing Service System (http://cdc.cma.gov.cn/). The mean annual maximum and
114 minimum temperature at the Bayanbulak meteorological station are 3.1 ℃ and
115 -10.6 ℃ and mean annual precipitation is 267 mm, and generally precipitation falls as
116 rain from May to September and as snow from October to April of the next year.

117 The observed streamflow data at the Dashankou hydrologic station (the triangle in
118 Fig. 1) are from Xinjiang Tarim River Basin Management Bureau. The average daily
119 flow is around 110 $m^3 s^{-1}$ (equivalent to 185 mm runoff per year), ranging from 15 m^3
120 s^{-1} to 973 $m^3 s^{-1}$.

121 2.2 Simulated meteorological variables from the RCM

122 GCM or RCM outputs are generally biased (Ahmed et al., 2013; Teutschbein and
123 Seibert, 2012; Mehrotra and Sharma, 2012), and there is a need to correct these outputs
124 before used for regional impact studies. The RCM outputs used in this study are based
125 on the work done by Gao et al. (2013), where the RCM outputs used in this study are

126 based on the work done by Gao et al. (2013). In Gao et al. (2013), the RCM model
127 (RegCM, Giorgi and Mearns, 1999) was driven by a global climate model
128 BCC_CSM1.1 (Beijing Climate Center Climate System Model; Wu et al., 2013; Xin et
129 al., 2013) at a horizontal resolution of 50 km over China.

130 The RCM outputs were validated with the observational dataset (CN05.1) over
131 China for the period from 1961 to 2005. The RCM outputs show reasonable simulation
132 of temperature and precipitation in most parts of China except some regions where our
133 study area is located (for more details refer to Gao et al., 2013).

134

135 **3 Methodology**

136 Figure 2 shows the flow chart of the comparison procedure. First, grid based
137 RCM simulation was downscaled to station scale using bias correction methods, and
138 then the corrected meteorological data were compared to the observation at these two
139 stations and to each other ("Meteorological data comparison" in Fig. 2). These station
140 based meteorological data were then upscaled to watershed scale with the precipitation
141 and temperature lapse rates before they were used to drive the hydrological model
142 (SWAT). Finally, the simulated streamflow driven by the corrected and observed
143 meteorological data were compared to observed streamflow and to each other
144 ("Streamflow comparison" in Fig. 2).

145 3.1 Hydrologic model and sensitivity analysis

146 SWAT (Soil and Water Assessment Tool; Arnold et al., 1998) is a distributed and
147 time continuous watershed hydrologic model. The climatic input (driving force)
148 consists of daily precipitation, maximum/minimum temperature, solar radiation, wind
149 speed and relative humidity. To account for orographic effects on precipitation and
150 temperature, elevation bands were used. Within each elevation band, the precipitation
151 and temperature are estimated based on their lapse rates and elevation. For more details,
152 refer to SWAT manuals (http://www.brc.tamus.edu/). SWAT has been being widely
153 used for comprehensive modeling of the impact of management practices and climate
154 change on the hydrologic cycle and water resources at a watershed scale (e.g., Arnold
155 et al., 2000; Arnold and Fohrer, 2005; Setegn et al., 2011).

156 In this study, SWAT model was firstly set up with available DEM, landuse, soil,
157 and observed climate data, and then model parameters were calibrated with the
158 observed streamflow data at the Dashankou Station. The simulation results show: 1)
159 model application shows excellent performances for both calibration period (1986 ~
160 1989) and validation period (1990 ~ 2001) with daily "NS"s (Nash-Sutcliffe
161 coefficients, Nash and Sutcliffe, 1970; see the definition in Eq. (16)) and "R^2"s over
162 0.80, which is highly acceptable; 2) model parameters are reasonable and spatial
163 patterns of precipitation and temperature are in agreement with other studies in the
164 region (see more details in Fang et al., 2015). Figure 3 shows a comparison of mean
165 hydrographs of the observed ("obs") and simulated flows ("default"). This calibrated
166 model hence provides a basis for evaluation of the impact of different correction

methods on streamflow.

To study the relative importance of the five meteorological variables, the Sobol' sensitivity analysis method (Sobol', 2001) was applied. The Sobol' method is based on the decomposition of the variance V of objective function:

$$V = \sum_i V_i + \sum_i \sum_{j>i} V_{ij} + \cdots + V_{1,2,\cdots,n} \quad (1)$$

where

$$V_i = V(\mu(Y|X_i))$$

$$V_{ij} = V\left(\mu\left(Y\middle|X_i, X_j\right)\right) - V_i - V_j$$

and so on. Herein, $V(.)$ denotes the variance operator, V is the total variance, and V_i and V_{ij} are main variance of X_i (the i^{th} factor of X) and partial variance of X_i and X_j. Here factors X are the changes applied to these five meteorological variables, respectively (see Table 1 for a list of these factors). In practice, normalized indices are often used as sensitivity measures:

$$S_i = \frac{V_i}{V}, 1 \le i \le n \quad (2)$$

$$S_{ij} = \frac{V_{ij}}{V}, 1 \le i < j \le n \quad (3)$$

$$S_{Ti} = S_i + \sum_j S_{ij} + \sum_j \sum_k S_{ijk} + \cdots + S_{1,2,\ldots,n}, \ 1 \le i \le n \quad (4)$$

Where S_i, S_{ij} and S_{Ti} are the main effect of X_i, first order interaction between X_i and X_j, and total effect of X_i. S_{Ti} ranges from 0 to 1 and denotes the importance of the factor to model output. The larger S_{Ti}, the more important this factor is. The difference between S_{Ti} and S_i denotes the significance of the interaction of this factor with other factors. As a result, the larger this difference, the more significant the interaction is.

3.2 Bias correction methods

In this study, five bias correction methods were used for precipitation, and three for temperature. These methods are listed in Table 2. All these bias correction methods were conducted on a daily basis from 1975 to 2005.

3.2.1 Linear Scaling (LS) of precipitation and temperature

LS method aims to perfectly match the monthly mean of corrected values with that of observed ones (Lenderink et al., 2007). It operates with monthly correction values based on the differences between observed and raw data (raw RCM simulated data in this case). Precipitation is typically corrected with a multiplier and temperature with an additive term on a monthly basis:

$$P_{cor,m,d} = P_{raw,m,d} \times \frac{\mu(P_{obs,m})}{\mu(P_{raw,m})} \quad (5)$$

$$T_{cor,m,d} = T_{raw,m,d} + \mu(T_{obs,m}) - \mu(T_{raw,m}) \quad (6)$$

where $P_{cor,m,d}$ and $T_{cor,m,d}$ are corrected precipitation and temperature on the d^{th} day of m^{th} month and $P_{raw,m,d}$ and $T_{raw,m,d}$ are the raw precipitation and temperature on the d^{th} day of m^{th} month. $\mu(.)$ represents the expectation operator (e.g., $\mu(P_{obs,m})$ represents the mean value of observed precipitation at given month *m*).

3.2.2 LOCal Intensity scaling (LOCI) of precipitation

LOCI method (Schmidli et al., 2006) corrects the wet-day frequencies and intensities and can effectively improve the raw data which have too many drizzle days (days with little precipitation). It normally involves two steps: firstly, a wet-day threshold for the m^{th} month $P_{thres,m}$ is determined from the raw precipitation series to

ensure that the threshold exceedance matches the wet-day frequency of the observation; secondly, a scaling factor $s_m = \frac{\mu(P_{obs,m,d}|P_{obs,m,d}>0)}{\mu(P_{raw,m,d}|P_{raw,m,d}>P_{thres,m})}$ is calculated and used to ensure that the mean of the corrected precipitation is equal to that of the observed precipitation:

$$P_{cor,m,d} = \begin{cases} 0, & if\ P_{raw,m,d} < P_{thres,m} \\ P_{raw,m,d} \times S_m, & otherwise \end{cases} \quad (7)$$

3.2.3 Power Transformation (PT) of precipitation

While the LS and LOCI account for the bias in the mean precipitation, it does not correct biases in the variance. PT method uses an exponential form to further adjust the standard deviation of precipitation series. Since PT has the limitation in correcting the wet day probability (Teutschbein and Seibert, 2012), which was also confirmed in our study (not shown), LOCI method is applied to correct precipitation prior to the correction by PT method.

Therefore, to implement this PT method, firstly, we estimate b_m that minimizes:

$$\mathrm{f}(b_m) = \frac{\sigma(P_{obs,m})}{\mu(P_{obs,m})} - \frac{\sigma(P_{LOCI,m}^{b_m})}{\mu(P_{LOCI,m}^{b_m})} \quad (8)$$

where b_m is the exponent for the m^{th} month, $\sigma(.)$ represents the standard deviation operator, and $P_{LOCI,m}$ is the LOCI-corrected precipitation in the m^{th} month. If b_m is larger than one, it indicates that the LOCI-corrected precipitation underestimates its coefficient of variance in month m.

After finding the optimal b_m, the parameter $s_m = \frac{\mu(P_{obs,m})}{\mu(P_{LOCI,m}^{b_m})}$ is then determined such that the mean of the corrected values corresponds to the observed mean. The corrected precipitation series are obtained based on the LOCI corrected precipitation

$P_{cor,m,d}$:

$$P_{cor,m,d} = s_m \times P_{LOCI,m,d}^{b_m} \quad (9)$$

3.2.4 VARIance scaling (VARI) of temperature

The PT method is an effective method to correct both the mean and variance of precipitation, but it cannot be used to correct temperature time series, as temperature is known to be approximately normally distributed (Terink et al., 2010). VARI method was developed to correct both the mean and variance of normally distributed variable such as temperature (Teutschbein and Seibert, 2012; Terink et al., 2010). Temperature is normally corrected using VARI method with Eq. (10).

$$T_{cor,m,d} = \left[T_{raw,m,d} - \mu\left(T_{raw,m}\right)\right] \times \frac{\sigma\left(T_{obs,m}\right)}{\sigma\left(T_{raw,m}\right)} + \mu\left(T_{obs,m}\right) \quad (10)$$

3.2.5 Distribution Mapping (DM) of precipitation and temperature

DM method is to match the distribution function of raw data to that of observation. It is used to adjust mean, standard deviation and quantiles. Furthermore, it preserves the extremes (Themeßl et al., 2012). However, it also has its limitation due to the assumption that both the observed and raw meteorological variables follow the same proposed distribution, which may introduce potential new biases.

For precipitation, the Gamma distribution (Thom, 1958) with shape parameter α and scale parameter β is often used for precipitation distribution and has been proven to be effective (e.g., Block et al., 2009; Piani et al., 2010):

$$f_r(x|\alpha,\beta) = x^{\alpha-1} \times \frac{1}{\beta^{\alpha} \times \Gamma(\alpha)} \times e^{\frac{-x}{\beta}}; x \geq 0, \alpha, \beta > 0 \quad (11)$$

where $\Gamma(.)$ is the Gamma function. Since the raw RCM-simulated precipitation contains a large number of drizzle days, which may substantially distort the raw precipitation distribution, the correction is done on LOCI corrected precipitation $P_{LOCI,m,d}$:

$$P_{cor,m,d} = F_r^{-1}\left(F_r\left(P_{LOCI,m,d}\middle|\alpha_{LOCI,m},\beta_{LOCI,m}\right)\middle|\alpha_{obs,m},\beta_{obs,m}\right) \quad (12)$$

Where $F_r(.)$ and $F_r^{-1}(.)$ are Gamma CDF (cumulative distribution function) and its inverse. $\alpha_{LOCI,m}$ and $\beta_{LOCI,m}$ are the fitted Gamma parameter for the LOCI corrected precipitation in a given month m, and $\alpha_{obs,m}$ and $\beta_{obs,m}$ are these for observation.

For temperature, the Gaussian distribution (or normal distribution) with mean μ and standard deviation σ is usually assumed to fit temperature best (Teutschbein and Seibert, 2012):

$$f_N(x|\mu,\sigma) = \frac{1}{\sigma\times\sqrt{2\pi}} \times e^{\frac{-(x-\mu)^2}{2\sigma^2}}; x \in \mathbf{R} \quad (13)$$

And then similarly the corrected temperature can be expressed as:

$$T_{cor,m,d} = F_N^{-1}\left(F_N\left(T_{raw,m,d}\middle|\mu_{raw,m},\sigma_{raw,m}\right)\middle|\mu_{obs,m},\sigma_{obs,m}\right) \quad (14)$$

where $F_N(.)$ and $F_N^{-1}(.)$ are Gaussian CDF and its inverse, $\mu_{raw,m}$ and $\mu_{obs,m}$ are the fitted and observed means for the raw and observed precipitation series at a given month m, and $\sigma_{raw,m}$ and $\sigma_{obs,m}$ are the corresponding standard deviations, respectively.

3.2.6 Quantile Mapping (QM) of precipitation

QM method is a non-parametric bias correction method and is generally

applicable for all possible distributions of precipitation without any assumption on precipitation distribution. This approach originates from the empirical transformation (Themeßl et al., 2012) and was successfully implemented in the bias correction of RCM simulated precipitation (Sun et al., 2011; Themeßl et al., 2012; Chen et al., 2013a; Wilcke et al., 2013). It can effectively correct bias in the mean, standard deviation and wet day frequency as well as quantiles.

For precipitation, the adjustment of precipitation using QM can be expressed in terms of the empirical CDF (*ecdf*) and its inverse ($ecdf^{-1}$):

$$P_{cor,m,d} = ecdf_{obs,m}^{-1}\left(ecdf_{raw,m}\left(P_{raw,m,d}\right)\right) \quad (15)$$

3.3 Performance evaluation

The performance evaluation of these correction methods is based on their abilities to reproduce precipitation, temperature, and streamflow simulated with a hydrological model (SWAT) driven by bias corrected RCM simulations. When evaluating ability to reproduce streamflow, streamflow is firstly simulated by running the hydrological model driven by 15 different combinations of corrected precipitation, max/min temperature with different correction methods (these hydrologic simulations are then referred to as simulations 1 to 15, which are listed in Table 3) together with hydrologic simulations driven by observed meteorological data ("default") and raw RCM simulation ("raw"). These 15 simulations were then compared with observed streamflows and "default" and "raw".

297 The performance evaluation of precipitation, temperature and streamflow are as
298 follows.

299 1) For corrected precipitation, frequency-based indices and time series
300 performances are compared with observed precipitation data. The frequency-based
301 indices include mean, median, standard deviation, 99th percentile, probability of wet
302 days, and intensity of wet day while time-series based metrics include Nash-Sutcliffe
303 coefficient(NS), Percent bias (P_{BIAS}), R^2 and Mean Absolute Error (MAE) defined as
304 follows:

305 $$NS = 1 - \frac{\sum_{i=1}^{n}\left(Y_i^{obs} - Y_i^{sim}\right)^2}{\sum_{i=1}^{n}\left(Y_i^{obs} - Y^{mean}\right)^2} \quad (16)$$

306 $$P_{BIAS} = \frac{\sum_{i=1}^{n}\left(Y_i^{obs} - Y_i^{sim}\right)}{\sum_{i=1}^{n}\left(Y_i^{obs}\right)} \quad (17)$$

307 $$MAE = \frac{\sum_{i=1}^{n}\left|Y_i^{obs} - Y_i^{sim}\right|}{n} \quad (18)$$

308 Where Y_i^{obs} and Y_i^{sim} are the i^{th} observed and simulated variables, Y^{mean} is the mean of
309 observed variables, and *n* is the total number of observations.

310 NS indicates how well the simulation matches the observation and it ranges
311 between -∞ and 1, with NS =1 meaning a perfect fit. The higher this value, the more
312 reliable the model is in comparison to the mean. P_{BIAS} measures the average tendency
313 of the simulated data to their observed counterparts. Positive values indicate an
314 overestimation of observation, while negative values indicate an underestimation. The
315 optimal value of P_{BIAS} is 0.0, with low-magnitude values indicating accurate model
316 simulations. MAE demonstrates the average model prediction error with less
317 sensitivity to large errors.

318 2) For corrected temperature, frequency-based indices and time series

performances are compared with observed temperature data. The frequency-based indices include mean, median, standard deviation, and 10^{th}, 90^{th} percentile while time-series based metrics include NS, P_{BIAS}, R^2 and MAE.

3) For simulated streamflow driven by corrected RCM simulations, the frequency-based indices are visualized using boxplot, exceedance probability curve. Time-series based metrics include NS, P_{BIAS}, R^2 and MAE.

4 Results and discussion

4.1. Initial streamflow simulation driven with raw RCM simulations and sensitivity analysis

To illustrate the necessity of bias correction in climate change impact on hydrology, we re-calibrated SWAT using the raw RCM simulations while keeping all SWAT parameters in their reasonable ranges. The assumption is that if the re-calibrated hydrological model driven by the raw RCM simulations performs well and model parameters are reasonable, then there is no need for bias correction. The streamflow simulated by the re-calibrated model was plotted in Fig. 3, and it systematically overestimates the observation with NS equals to -6.65. Therefore, it is necessary to correct the meteorological variables before they can be used for a hydrological impact study.

The Sobol' method was applied to study which meteorological variables should be corrected for hydrological modeling. Table 1 lists the sensitivity results for these five

meteorological variables. As can be seen, precipitation is the most sensitive factor (the main effect S_i is 44.0% and total effect S_{Ti} is 74.0%), followed by temperature (S_i = 15.0% and S_{Ti} = 36.9%) and solar radiation (S_i = 7.7% and S_{Ti} = 22.6%), and the interactions between these factors are large. Relative humidity and wind speed are insensitive in this case. This means precipitation, temperature and solar radiation need to be bias corrected before applied to hydrologic models, while relative humidity and wind speed over the region do not need any correction.

4.2 Evaluation of corrected precipitation and temperature

The bias correction was done on RCM simulated precipitation, max/min temperature, and solar radiation (for solar radiation, LS and VARI methods were used) for two meteorological stations Bayanbulak and Baluntai. Results show: 1) for solar radiation, there is no significant difference for different correction methods. There the results are not shown. 2) Similar results were obtained for minimum temperature and maximum temperature, and for Bayanbulak and Baluntai. Therefore we only listed and discussed results for Bayanbulak, and maximum temperature.

Table 4 lists the frequency-based statistics of observed (“obs”), raw RCM-simulated (“raw”) and corrected (denoted by the corresponding correction method) precipitation data at the Bayanbulak Station. This station has a daily mean precipitation of 0.73 mm or annual mean of 266 mm and precipitation falls in 32% days in a year with a mean intensity of 2.3 mm. Compared to the observation, the raw

RCM simulation deviates significantly from observation, with overestimation of all the statistics. All the bias correction methods improve the raw RCM simulated precipitation, however, there are differences in their corrected statistics. LS method has a good estimation of the mean while it shows a large bias in other measures, e.g., it largely overestimated the probability of wet days (e.g., up to 41% overestimation) and underestimated the standard deviation (up to 0.9 mm underestimation). LOCI method provides a good estimation in the mean, median, wet-day probability and wet-day intensity; however, there is a slight underestimation in the standard deviation and therefore 99^{th} percentile. Compared to LS and LOCI, PT method performs well in all these metrics. DM method has a slight overestimation of the mean and an underestimation of standard deviation. This means that precipitation does not follow the assumed Gamma distribution. On the contrary, QM method doesn't have this assumption and it provides an excellent estimation of these statistics. These results are consistent with previous studies (Themeßl et al., 2011, 2012; Wilcke et al., 2013; Graham et al., 2007), but are different from the research by Piani et al. (2010) who found that performance of DM method is unexpectedly well for the humid Europe region. This discrepancy can be partly attributed to the precipitation regime for different regions since better fit of the assumed distribution lead to better performance of DM.

Table 5 lists the frequency-based statistics of observed ("obs"), raw RCM simulated ("raw") and corrected (denoted by the corresponding method) maximum

temperature data at the Bayanbulak Station. The mean and standard deviation of "obs" are 3.1 and 14.5 ℃, with the 90th percentile being 19.2 ℃. Analysis of the "raw" indicates deviation from "obs", with an overestimation of the mean, and underestimations of the median, standard deviation, and 90th percentile. All three correction methods correct biases in the "raw" and improve estimations of the statistics. LS has a correct estimation of mean but slight underestimations of median and standard deviation, while VARI and DM have good estimations of all the frequency-based statistics. These results confirm the study by Teutschbein and Seibert (2012), i.e., LS method doesn't adjust the standard deviation and the percentiles while VARI and DM methods do.

Figure 4 shows the exceedance probability curves of the observed and corrected precipitation and temperature. For precipitation, the raw RCM simulations are heavily biased (as also shown by statistics in Table 4). All correction methods effectively, but in different extent, correct biases in raw precipitation. The LS method underestimates the high precipitation with probabilities below 0.06 and overestimates the low precipitation with probabilities between 0.06 ~ 0.32. The overestimation of precipitation with probabilities between 0.32 ~ 0.73 indicates LS method has a very limited ability in reproducing dry day precipitation (below 0.1 mm). Similar to LS method, the LOCI method also overestimates the low precipitation with probabilities between 0.08 ~ 0.32 and underestimates the high intensities with probabilities below 0.08, which is in line with previous arguments by Berg et al. (2012). However, unlike

LS method, LOCI method performs well on the estimation of the dry days with precipitation below 0.1 mm. The PT, DM and QM methods well adjust precipitation exceedance except that DM method slightly overestimates the precipitation with probabilities between 0.12 ~ 0.28. For temperature, the raw temperature overestimates low temperature with probabilities above 0.65 and underestimates high temperature with probabilities below 0.65. All temperature correction methods adjust the biases in raw temperature and the corrected temperature has similar quantile values with the observation. They performed equally well and differences among these correction methods are negligible.

Time-series based performances were evaluated and results are shown in Fig. 5 and Table 6. For precipitation, all bias correction methods significantly improve the raw RCM simulations. However, as shown in the right plot of Fig. 5, there is a systematic mismatch between observation and corrections which follow the pattern of the raw RCM simulated precipitation, which indicates that all bias correction methods fail to correct the temporal pattern of precipitation. In addition, this mismatch differs between different methods, among which the differences are smaller for LS and LOCI methods than for PT, DM and QM methods. This resulted in a slightly better squared difference based measures (e.g., NS, R^2) for LS and LOCI than PT, DM and QM methods, as is indicated in Table 6. Similar to precipitation, all correction methods significantly improved the raw RCM simulated temperature. Biases in raw temperature (e.g., 1.1 ℃ in spring, 1.0 ℃ in summer, 3.3 ℃ in autumn, and up to

427 7.6 ℃ in winter) were corrected. These three correction methods performed equally
428 well and no significant differences exist in terms of the average daily temperature
429 graphs.
430
431 Table 6 lists the time-series based metrics of corrected precipitation and
432 temperature at the Bayanbulak Station. For precipitation, the performance of the raw
433 RCM simulated precipitation is very poor with NS = -6.78, P_{BIAS} = 293.28% and MAE
434 = 65.40 mm for monthly data, and the improvements of correction are obvious. The
435 "P_{BIAS}"s of the corrected precipitation are within ± 7 % and "NS"s approach 0.64. It
436 is worth noting that LS and LOCI methods perform better than PT and QM methods in
437 terms of time series performances. For temperature, although the raw RCM simulation
438 obtains an acceptable NS value (0.84), it overestimates the observation with P_{BIAS} =
439 15.78% and MAE = 4.31 ℃. The "P_{BIAS}"s of the corrected temperatures are within
440 $\pm$5% and "NS"s are over 94% (better than that of the "raw") for all three correction
441 methods and there is no significant difference between these results, which indicates
442 the corrected monthly temperature series are in good agreement with the observation.
443

444 4.3 Evaluation of streamflow simulations

445 Figure 6 compares the mean, median, first and third quantiles of daily observed
446 streamflows ("obs"), simulated streamflows using observed meteorological inputs
447 ("default"), raw RCM simulations ("raw") and 15 combinations of corrected

precipitation and corrected temperature (i.e., simulations 1 to 15). The overestimation of simulated streamflow using raw RCM simulations (i.e., “raw”) is obvious. Simulations 1 to 3 overestimate streamflow with 100% overestimation of the mean streamflow while simulations 4 to 15 reproduce similar streamflows as the observation or simulation “default”. As the major difference between simulations 1 to 3 and other simulations is that simulations 1 to 3 use the LS-corrected precipitation, which means precipitation corrected with LS method has great bias in flow simulation in this study.

To investigate the performances of bias correction methods for different hydrological seasons, we divided the streamflow into two different periods according to the hydrograph (Fig. 3): wet period is from April to September and dry period is from October to March of next year. It indicates that the performances of bias correction methods are, except for magnitudes, similar for both wet and dry periods (not shown), which demonstrates that the evaluation is robust and can provide useful information for both dry and wet seasons.

Figure 7 shows the exceedance probability curves (flow duration curves) of the observed streamflow (“obs”), and streamflows with simulation “default” and simulations 4 to 15. For plotting purpose, simulations “raw” and 1 to 3 are not shown. Generally all simulations are in good agreement with the observation with probabilities between 0.12 and 0.72, and precipitation correction methods have more significant influence than temperature correction methods. This confirms the previous sensitivity results that precipitation is the most sensitive driving force in streamflow simulation. Similar to performances of bias corrected precipitation, simulations with DM corrected

precipitation (i.e. simulations 10 to 12) and LOCI corrected precipitation (i.e., simulations 4 to 6) deviate the observation the most, followed these with PT and QM methods. All simulations encounter the problem to correctly mimic the low flow part (i.e. probabilities larger than 0.7). This might be a systematic problem of the calibrated hydrologic model (as indicated by simulation "default"), e.g., the objective function of the hydrological modeling is not focused on baseflow. Differences among streamflows driven by different temperature but same precipitation are insignificant, which is different from the study of Teutschbein and Seibert (2012). This may be related to the watershed characteristic.

The performances of simulation "raw", simulations 1 to 15 at daily and monthly time steps (simulation "default" is taken as reference) are summarized in Table 3. The "raw" is heavily biased with NS close to -56.3 and P_{BIAS} as large as 399 % for monthly data. All the 15 simulations improve the statistics significantly. For simulations 1 to 3, whose precipitation series are corrected by LS method, NS ranges from -3.09 to -2.85 for monthly streamflow and they substantially overestimate the streamflow with P_{BIAS} over 100 %. For simulations 4 to 15, monthly "NS"s are over 0.60, which indicates they can reproduce satisfactory monthly streamflows in this watershed, and simulations with precipitation corrected by LOCI (simulations 4 to 6) have best "NS"s and "P_{BIAS}"s. However, these indices of are lower for daily streamflow ("NS"s range from 0.38 to 0.50), and this is related to the mismatch between corrected and observed precipitation time series (see top plot in Fig. 5), which is intrinsic from the RCM model and cannot be improved through these correction methods.

492 It is worth noting that simulations 1 to 3 and simulations 4 to 6, whose
493 precipitation is corrected by LS and LOCI, respectively, vary significantly. The
494 difference between LS and LOCI is that LOCI introduces a threshold for precipitation
495 on wet days to correct the wet day probability while LS doesn't. That is a simple but
496 quite pragmatic approach since the raw RCM simulated precipitation usually has too
497 many drizzle days (Teutschbein and Seibert, 2012). Obviously, wet day probability is
498 crucial to streamflow simulation when using elevation bands to account for spatial
499 variation in SWAT (see more details in SWAT manual, http://www.brc.tamus.edu/).
500 Figure 8 shows the monthly mean streamflow and exceedance probability curves
501 of 7-day peak and 7-day low flow. For the monthly mean streamflow, obviously the
502 "raw" is heavily biased with deviations ranging from 282% to 426%. Simulations 1 to
503 3 also overestimate the observation and the "default" as discussed before, while
504 simulations 4 to 15 reproduced good monthly mean streamflow. The annual peak flow
505 and low flow are presented in Fig. 8 to investigate the impact of bias correction
506 methods on extreme flows. For the peak flow, the exceedance probabilities of the
507 simulations 4 to 15 are close to the observation while "raw" and simulations 1 to 3
508 deviate significantly (not shown). It is worth noting that simulations 4, 5 and 6, which
509 perform the best in terms of the "NS"s, underestimate the peak flow by 1% ~ 28%. The
510 reason may be that the LOCI method adjusts all precipitation events in a certain month
511 with a same scaling factor, which leads to the underestimation of the standard
512 deviation and high precipitation intensity (Table 4), and finally results in an
513 underestimation of the peak streamflow. For the low flow, all simulations overestimate

514 the observation, but are in good agreement with the “default”, which can be attributed
515 to the systematic deficit in the hydrological model. DM method slightly overestimates
516 both peak flow and low flow. Results show slightly better performance of PT and QM
517 methods than LOCI and DM in predicting extreme flood and low flow, which is
518 consistent with previous studies in North America and Europe (e.g., Chen et al., 2013a;
519 Teutschbein and Seibert, 2012).
520

521 **5 Conclusions**

522 The work presented in this study compared the abilities of five precipitation and
523 three temperature correction methods in downscaling RCM simulations. The
524 downscaled meteorological data were then used to model hydrologic processes in an
525 arid region in China. The evaluation of the correction methods includes their abilities
526 to reproduce precipitation, temperature and streamflow using a hydrological model
527 driven by corrected meteorological variables. Several conclusions can be drawn:
528 1) Sensitivity analysis shows precipitation is the most sensitive driving force in
529 streamflow simulation, followed by temperature and solar radiation, while relative
530 humidity and wind speed are not sensitive.
531 2) Raw RCM simulations are heavily biased from observed meteorological data,
532 and this results in biases in the simulated streamflows which cannot be corrected
533 through calibration of the hydrological model. However all bias correction methods
534 effectively improve precipitation, temperature, and streamflow simulations.

3) Different precipitation correction methods show a big difference in downscaled precipitations while different temperature correction methods show similar results in downscaled temperatures. For precipitation, the PT and QM methods performed equally best in terms of the frequency-based indices; while LOCI method performed best in terms of the time-series based indices.

4) For simulated streamflow, precipitation correction methods have more significant influence than temperature correction methods and their performances on streamflow simulations are consistent with these of corrected precipitation, i.e., PT and QM methods performed equally best in correcting flow duration curve and peak flow while LOCI method performed best in terms of the time-series based indices. Note the LOCI and DM methods should be used with caution when analyzing drought or extreme streamflows because the LOCI method may underestimate the extreme precipitation and DM method performs ineffectively when either simulated precipitation or observed precipitation does not follow the proposed distribution. Besides, LS method is not suitable in hydrological impact assessment where there is a large variation in precipitation distribution when few meteorological stations are used since LS fails to correct wet day probability.

Generally, selection of precipitation correction method is more important than the selection of temperature correction method to downscale GCM/RCM simulations and thereafter for streamflow simulations. This might be generally true for other regional studies as GCMs/RCMs normally tend to better represent the temperature field than the precipitation field. However, the selection of precipitation correction method will be

case dependent. The comparison procedure listed in Figure 2 could be applied for other cases.

Acknowledgment

The research was supported by the "Thousand Youth Talents" Plan (Xinjiang Project) and the National Natural Science Foundation of China (41471030) and the Foundation of State Key Laboratory of Desert and Oasis Ecology (Y371163). We would like to thank Prof. Xuejie Gao at National Climate Center (China) for providing the output of Regional Climate Model used in this paper. The authors would like to thank reviewer Dr. Markus Muerth and an anonymous reviewer for their valuable comments and suggestions.

References

Ahmed, K. F., Wang, G., Silander, J., Wilson, A. M., Allen, J. M., Horton, R., and Anyah, R.: Statistical downscaling and bias correction of climate model outputs for climate change impact assessment in the US northeast, Global Planet Change, 100, 320-332, 2013.

Anderson, W. P., Jr., Storniolo, R. E., and Rice, J. S.: Bank thermal storage as a sink of temperature surges in urbanized streams, J Hydrol, 409, 525-537, 10.1016/j.jhydrol.2011.08.059, 2011.

Arnell, N. W.: Factors controlling the effects of climate change on river flow regimes in a humid temperate environment, J Hydrol, 132, 321-342, http://dx.doi.org/10.1016/0022-1694(92)90184-W, 1992

Arnold, J., Muttiah, R., Srinivasan, R., and Allen, P.: Regional estimation of base flow and groundwater recharge in the Upper Mississippi river basin, J Hydrol, 227, 21-40, 2000.

Arnold, J. G., Srinivasan, R., Muttiah, R. S., and Williams, J.: Large area hydrologic modeling and assessment part I: Model development1, JAWRA Journal of the American Water Resources Association, 34, 73-89, 1998.

585 Arnold, J. G., and Fohrer, N.: SWAT2000: current capabilities and research opportunities in applied
586 watershed modelling, Hydrol Process, 19, 563-572, 10.1002/hyp.5611, 2005.
587 Berg, P., Feldmann, H., and Panitz, H. J.: Bias correction of high resolution regional climate model data,
588 J Hydrol, 448, 80-92, 2012.
589 Bergstrom, S., Carlsson, B., Gardelin, M., Lindstrom, G., Pettersson, A., and Rummukainen, M.:
590 Climate change impacts on runoff in Sweden-assessments by global climate models, dynamical
591 downscaling and hydrological modelling, Climate Res, 16, 101-112, 2001.
592 Block, P. J., Souza Filho, F. A., Sun, L., and Kwon, H. H.: A Streamflow Forecasting Framework using
593 Multiple Climate and Hydrological Models1, JAWRA Journal of the American Water Resources
594 Association, 45, 828-843, 2009.
595 Buytaert, W., Vuille, M., Dewulf, A., Urrutia, R., Karmalkar, A., and Celleri, R.: Uncertainties in climate
596 change projections and regional downscaling in the tropical Andes: implications for water resources
597 management, Hydrol Earth Syst Sc, 14, 1247-1258, 10.5194/hess-14-1247-2010, 2010.
598 Chen, J., Brissette, F. P., Chaumont, D., and Braun, M.: Finding appropriate bias correction methods in
599 downscaling precipitation for hydrologic impact studies over North America, Water Resour Res, 49,
600 4187-4205, 10.1002/wrcr.20331, 2013a.
601 Chen, Y., Xu, C., Chen, Y., Li, W., and Liu, J.: Response of glacial-lake outburst floods to climate
602 change in the Yarkant River basin on northern slope of Karakoram Mountains, China, Quaternary
603 International, 226, 75-81, 2010.
604 Chen, Y., Du, Q., and Chen, Y.: Sustainable water use in the Bosten Lake Basin, Science press, Beijing,
605 329 pp., 2013b.
606 Chen, Z., Chen, Y., and Li, B.: Quantifying the effects of climate variability and human activities on
607 runoff for Kaidu River Basin in arid region of northwest China, Theoretical and applied
608 climatology, 111, 537-545, 2013c.
609 Elguindi, N., Somot, S., Déqué, M., and Ludwig, W.: Climate change evolution of the hydrological
610 balance of the Mediterranean, Black and Caspian Seas: impact of climate model resolution, Clim
611 Dynam, 36, 205-228, 2011.
612 Fang, G., Yang, J., Chen, Y., Xu, C.: Contribution of meteorological input in calibrating a distributed
613 hydrologic model with the application to a watershed in the Tianshan Mountains, China, Environ
614 Earth Sci, 10.1007/s12665-015-4244-7, 2015.
615 Fowler, H. J., Ekström, M., Blenkinsop, S., and Smith, A. P.: Estimating change in extreme European
616 precipitation using a multimodel ensemble, J Geophys Res, 112, D18, 2007.
617 Gao, X., Wang, M., and Giorgi, F.: Climate change over China in the 21st century as simu-lated by
618 BCC_CSM1. 1-RegCM4. 0, Atmos. Oceanic Sci. Lett, 6, 381-386, 2013.
619 Giorgi, F.: Simulation of regional climate using a limited area model nested in a general circulation
620 model, Journal of Climate 3, 941-963, 1990.
621 Giorgi, F., and Mearns, L. O.: Introduction to special section: Regional climate modeling revisited,
622 Journal of Geophysical Research: Atmospheres (1984–2012), 104, 6335-6352, 1999.
623 Graham, L. P., Andréasson, J., and Carlsson, B.: Assessing climate change impacts on hydrology from
624 an ensemble of regional climate models, model scales and linking methods–a case study on the
625 Lule River basin, Climatic Change, 81, 293-307, 2007.
626 Lenderink, G., Buishand, A., and Deursen, W. v.: Estimates of future discharges of the river Rhine using
627 two scenario methodologies: direct versus delta approach, Hydrol Earth Syst Sc, 11, 1145-1159,
628 2007.

Li, B., Chen, Y., and Shi, X.: Why does the temperature rise faster in the arid region of northwest China?, J Geophys Res, 117, 2012.

Liu, T., Willems, P., Pan, X. L., Bao, A. M., Chen, X., Veroustraete, F., and Dong, Q. H.: Climate change impact on water resource extremes in a headwater region of the Tarim basin in China, Hydrol Earth Syst Sc, 15, 3511-3527, 10.5194/hess-15-3511-2011, 2011.

Liu, Z., Xu, Z., Huang, J., Charles, S. P., and Fu, G.: Impacts of climate change on hydrological processes in the headwater catchment of the Tarim River basin, China, Hydrol Process, 24, 196-208, 10.1002/hyp.7493, 2010.

Maraun, D., Wetterhall, F., Ireson, A. M., Chandler, R. E., Kendon, E. J., Widmann, M., Brienen, S., Rust, H. W., Sauter, T., Themeßl, M., Venema, V. K. C., Chun, K. P., Goodess, C. M., Jones, R. G., Onof, C., Vrac, M., and Thiele-Eich, I.: Precipitation downscaling under climate change: recent developments to bridge the gap between dynamical models and the end user, Rev Geophys, 48, RG3003, 2010.

Mehrotra, R., and Sharma, A.: An improved standardization procedure to remove systematic low frequency variability biases in GCM simulations, Water Resour Res, 48, W12601, 10.1029/2012WR012446, 2012.

Murphy, J.: An evaluation of statistical and dynamical techniques for downscaling local climate, Journal of Climate, 12, 2256-2284, 1999.

Nash, J. E., and Sutcliffe, J.: River flow forecasting through conceptual models part I—A discussion of principles, J Hydrol, 10, 282-290, 1970.

Piani, C., Haerter, J., and Coppola, E.: Statistical bias correction for daily precipitation in regional climate models over Europe, Theoretical and Applied Climatology, 99, 187-192, 2010.

Schmidli, J., Frei, C., and Vidale, P. L.: Downscaling from GC precipitation: A benchmark for dynamical and statistical downscaling methods, International Journal of Climatology, 26, 679-689, 10.1002/joc.1287, 2006.

Seager, R., and Vecchi, G. A.: Greenhouse warming and the 21st century hydroclimate of southwestern North America, Proc. Natl. Acad. Sci. U. S. A., 107, 21277-21282, 10.1073/pnas.0910856107, 2010.

Setegn, S. G., Rayner, D., Melesse, A. M., Dargahi, B., and Srinivasan, R.: Impact of climate change on the hydroclimatology of Lake Tana Basin, Ethiopia, Water Resour Res, 47, W04511, 10.1029/2010WR009248, 2011.

Shen, Y., and Chen, Y.: Global perspective on hydrology, water balance, and water resources management in arid basins, Hydrol Process, 24, 129-135, 2010.

Sobol', I. M.: Global sensitivity indices for nonlinear mathematical models and their Monte Carlo estimates, Math Comput Simulat, 55, 271-280, 10.1016/s0378-4754(00)00270-6, 2001.

Sun, F., Roderick, M. L., Lim, W. H., and Farquhar, G. D.: Hydroclimatic projections for the Murray-Darling Basin based on an ensemble derived from Intergovernmental Panel on Climate Change AR4 climate models, Water Resour Res, 47, W00G02, 10.1029/2010wr009829, 2011.

Terink, W., Hurkmans, R., Torfs, P., and Uijlenhoet, R.: Evaluation of a bias correction method applied to downscaled precipitation and temperature reanalysis data for the Rhine basin, Hydrology & Earth System Sciences, 14, 687-703, 2010.

Teutschbein, C., and Seibert, J.: Bias correction of regional climate model simulations for hydrological climate-change impact studies: Review and evaluation of different methods, J Hydrol, 456, 12-29, 10.1016/j.jhydrol.2012.05.052, 2012.

Themeßl, M. J., Gobiet, A., and Leuprecht, A.: Empirical‐statistical downscaling and error correction

of daily precipitation from regional climate models, International Journal of Climatology, 31, 1530-1544, 2011.

Themeßl, M. J., Gobiet, A., and Heinrich, G.: Empirical-statistical downscaling and error correction of regional climate models and its impact on the climate change signal, Climatic Change, 112, 449-468, 2012.

Thom, H. C.: A note on the gamma distribution, Mon Weather Rev, 86, 117-122, 1958.

Wang, H., Chen, Y., Li, W., and Deng, H.: Runoff responses to climate change in arid region of northwestern China during 1960–2010, Chinese Geographical Science, 23, 286-300, 2013.

Wilcke, R. A. I., Mendlik, T., and Gobiet, A.: Multi-variable error correction of regional climate models, Climatic Change, 120, 871-887, 2013.

Wu, T., Li, W., Ji, J., Xin, X., Li, L., Wang, Z., Zhang, Y., Li, J., Zhang, F., and Wei, M.: Global carbon budgets simulated by the Beijing Climate Center Climate System Model for the last century, Journal of Geophysical Research: Atmospheres, 118, 4326-4347, 2013.

Xin, X., Wu, T., Li, J., Wang, Z., Li, W., and Wu, F.: How well does BCC_CSM1. 1 reproduce the 20th century climate change over China, Atmos. Oceanic Sci. Lett, 6, 21-26, 2013.

Xu, C., Chen, Y., Chen, Y., Zhao, R., and Ding, H.: Responses of Surface Runoff to Climate Change and Human Activities in the Arid Region of Central Asia: A Case Study in the Tarim River Basin, China, Environ Manage, 51, 926-938, 2013.

697

698 **Table 1.** Sensitivity indices of the five meteorological variables based on the Sobol' method.

Factor[a]	Meaning	Factor Range	Main effect S_i (%)	Total effect S_{Ti} (%)
a__tmp	Additive change to temperature	[-5,5]	15.0	36.9
r__pcp	Relative change to precipitation	[-0.5,0.5]	44.0	74.0
r__hmd	Relative change to humidity	[-0.5,0.5]	0.0	0.0
r__slr	Relative change to solar radiation	[-0.5,0.5]	7.7	22.6
r__wnd	Relative change to wind speed	[-0.5,0.5]	0.3	0.9

699 [a] Here, '*a__*' or '*r__*' means an addictive or a relative change to the initial parameter values.

700

Table 2. Bias correction methods for RCM-simulated precipitation and temperature.

Bias correction for precipitation	Bias correction for temperature
Linear Scaling (LS)	Linear Scaling (LS)
LOCal Intensity scaling (LOCI)	VARIance scaling (VARI)
Power Transformation (PT)	Distribution Mapping for temperature using Gaussian distribution (DM)
Distribution Mapping for precipitation using Gamma distribution (DM)	
Quantile Mapping (QM)	

704

705 **Table 3.** Performances of simulated streamflows driven by raw RCM simulated ("raw") and 15
706 combinations of bias-corrected precipitation and temperature (denoted as numbers from 1 to 15)
707 compared to the simulation driven by observed climate ("default") during the period 1986 ~ 2001.
708 For simulations 1 to 15, solar radiation is corrected with Linear Scaling (LS) method.

709

Bias correction method			Daily				Monthly			
	Precipitation	Temperature	NS (-)	P_{BIAS} (%)	R^2 (-)	MAE (m^3/s)	NS (-)	P_{BIAS} (%)	R^2 (-)	MAE (m^3/s)
raw	raw	raw	-47.69	398.9	0.4	547.5	-56.34	399.4	0.6	524.6
1	LS	LS	-2.66	106.2	0.5	150.1	-3.09	106.4	0.7	140.2
2	LS	VARI	-2.43	103.5	0.5	145.4	-2.85	103.7	0.7	135.9
3	LS	DM	-2.43	103.5	0.5	145.4	-2.85	103.7	0.7	135.9
4	LOCI	LS	0.49	-8.0	0.5	56.0	0.70	-7.9	0.7	38.2
5	LOCI	VARI	0.50	-8.6	0.5	55.6	0.70	-8.6	0.7	38.1
6	LOCI	DM	0.50	-8.6	0.5	55.6	0.70	-8.6	0.7	38.1
7	PT	LS	0.38	-3.3	0.4	61.7	0.64	-3.3	0.7	41.4
8	PT	VARI	0.39	-4.1	0.5	61.3	0.65	-4.1	0.7	41.1
9	PT	DM	0.39	-4.1	0.5	61.3	0.65	-4.1	0.7	41.1
10	DM	LS	0.41	3.6	0.5	60.3	0.66	3.6	0.7	40.5
11	DM	VARI	0.42	2.8	0.5	59.5	0.67	2.9	0.7	40.0
12	DM	DM	0.42	2.8	0.5	59.5	0.67	2.9	0.7	40.0
13	QM	LS	0.39	-2.6	0.5	61.3	0.65	-2.6	0.7	40.9
14	QM	VARI	0.40	-3.4	0.5	60.8	0.65	-3.4	0.7	40.7
15	QM	DM	0.40	-3.4	0.5	60.8	0.65	-3.4	0.7	40.7

710

711

712 **Table 4.** Frequency-based statistics of daily observed ("obs"), raw RCM-simulated ("raw") and

713 bias-corrected precipitations at the Bayanbulak Station

	Mean (mm)	Median (mm)	Standard deviation (mm)	99^{th} percentile (mm)	Probability of wet days (%)	Intensity of wet day (mm)
obs	0.73	0.0	2.4	12.4	32	2.3
raw	2.87	1.4	4.1	19.7	86	3.3
LS	0.73	0.2	1.5	7.6	73	1.0
LOCI	0.73	0.0	1.7	8.1	32	2.3
PT	0.73	0.0	2.4	11.4	32	2.3
DM	0.78	0.0	2.3	11.5	32	2.5
QM	0.73	0.0	2.4	12.4	32	2.3

714

715

716

717

718 **Table 5.** Frequency-based statistics (unit: ℃) of daily observed ("obs"), raw RCM simulated

719 ("raw") and bias corrected maximum temperatures at the Bayanbulak Station

	Mean	Median	Standard deviation	10^{th} percentile	90^{th} percentile
obs	3.08	7.20	14.50	-18.70	19.20
raw	3.45	3.21	10.88	-10.34	17.90
LS	3.08	6.65	14.14	-17.33	19.40
VARI	3.08	6.85	14.50	-17.76	19.36
DM	3.08	6.85	14.50	-17.76	19.36

720

721

722

723

724 **Table 6.** Time-series based metrics of bias-corrected precipitation and temperature calculated on a

725 monthly scale at the Bayanbulak Station

		NS (-)	P_{BIAS} (%)	R^2 (-)	MAE (mm or ℃)
Precipitation	raw	-6.78	293.28	0.42	65.40
	LS	0.64	0.06	0.65	9.66
	LOCI	0.61	-0.71	0.64	10.14
	PT	0.42	-0.09	0.53	11.98
	DM	0.46	6.64	0.56	11.78
	QM	0.44	0.03	0.54	11.99
Temperature	raw	0.84	15.78	0.88	4.31
	LS	0.95	3.04	0.95	2.35
	VARI	0.94	4.78	0.94	2.52
	DM	0.94	4.74	0.94	2.52

726

727

728

729

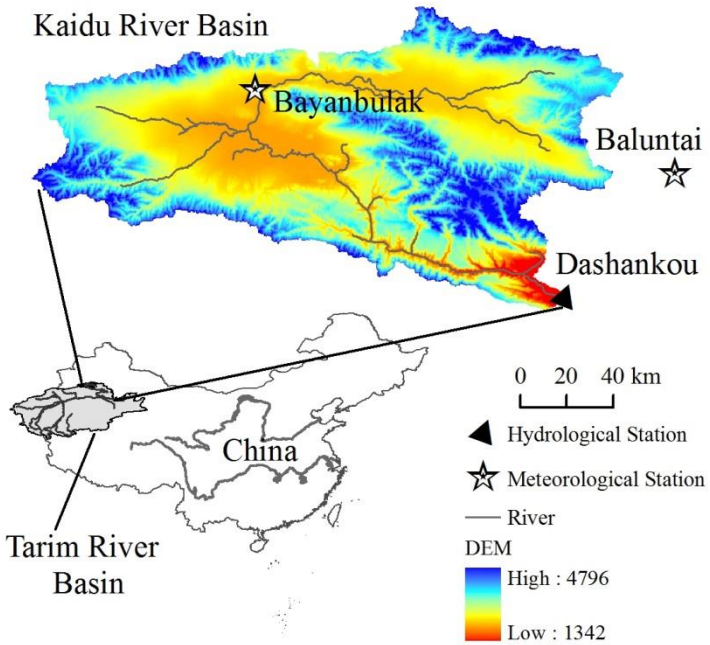

730

731 **Fig. 1.** Location of the study area, two meteorological stations and one hydrological station.

732

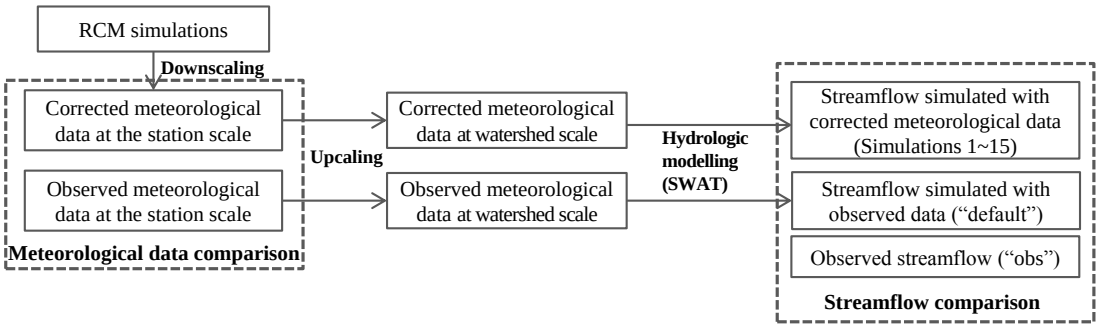

Fig. 2. Flow chart of comparison procedure

737

738

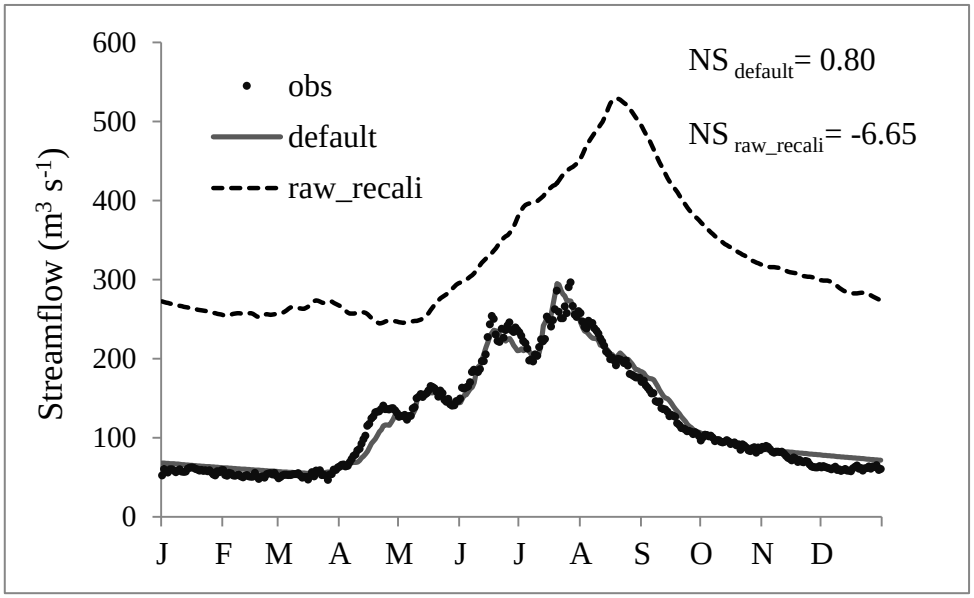

739

740 **Fig. 3.** Mean annual hydrographs of observed streamflow ("obs") and simulated streamflow using
741 observed meteorological data ("default") during the period of 1986 ~ 2001 at the Dashankou
742 Station. The simulated streamflow using raw RCM-simulated meteorological data after
743 re-calibration ("raw_recali") is also plotted. The NS values are for the daily continuous data and not
744 for the mean hydrograph.

745

746

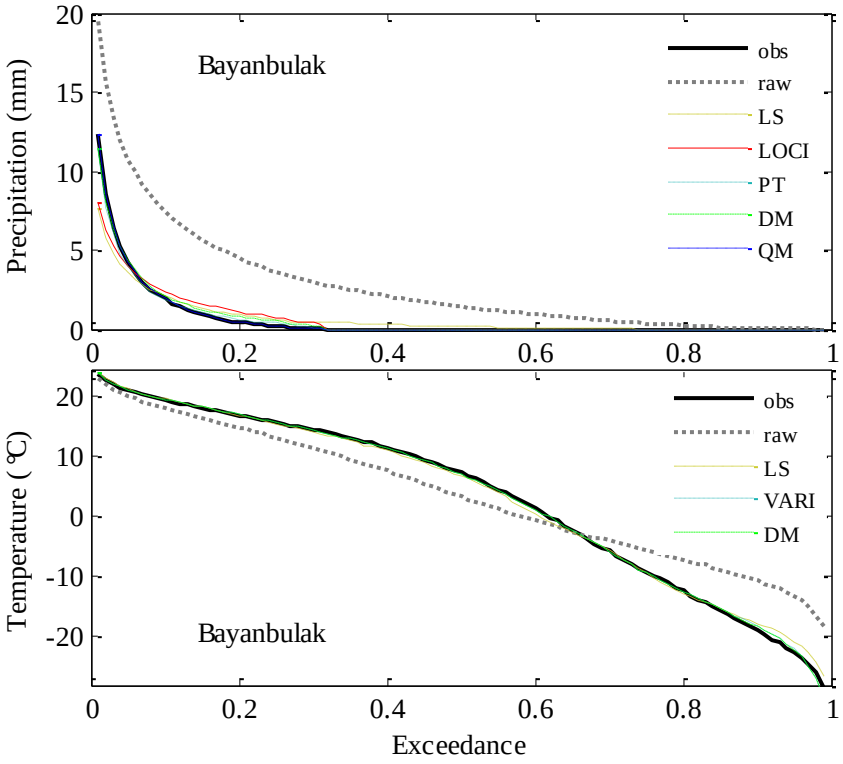

Fig. 4. Exceedance probabilities of the observed ("obs"), raw, and bias-corrected precipitation (top) and temperature (bottom) at the Bayanbulak Station.

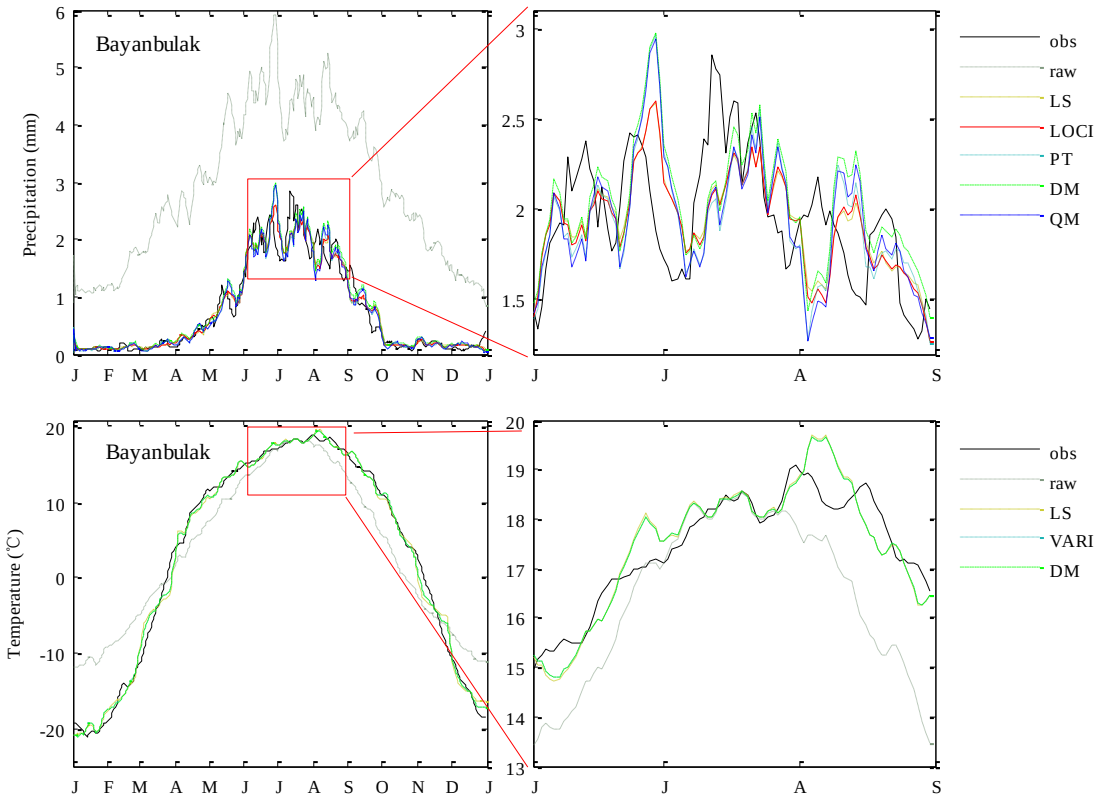

753

754 **Fig. 5.** Daily mean precipitation and temperature of observed ("obs"), raw RCM simulated ("raw"),
755 and bias corrected values at Bayanbulak Station, which were smoothed with 7-day moving average
756 method. The precipitation and temperature during May to August is amplified to inspect the
757 performance of each correction method.

758

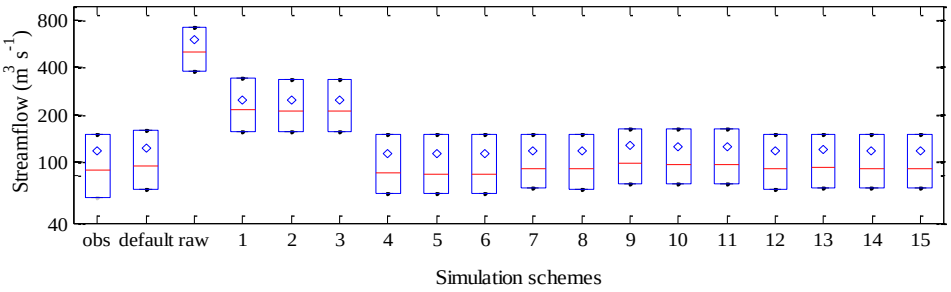

759

760 **Fig. 6.** Box plots of observed (“obs”) and simulated daily streamflows using observed (”default”),
761 raw RCM-simulated (“raw”) and corrected meteorological data (setup of simulations 1to 15 are
762 listed in Table 3). The mean values are shown with diamonds.

763

764

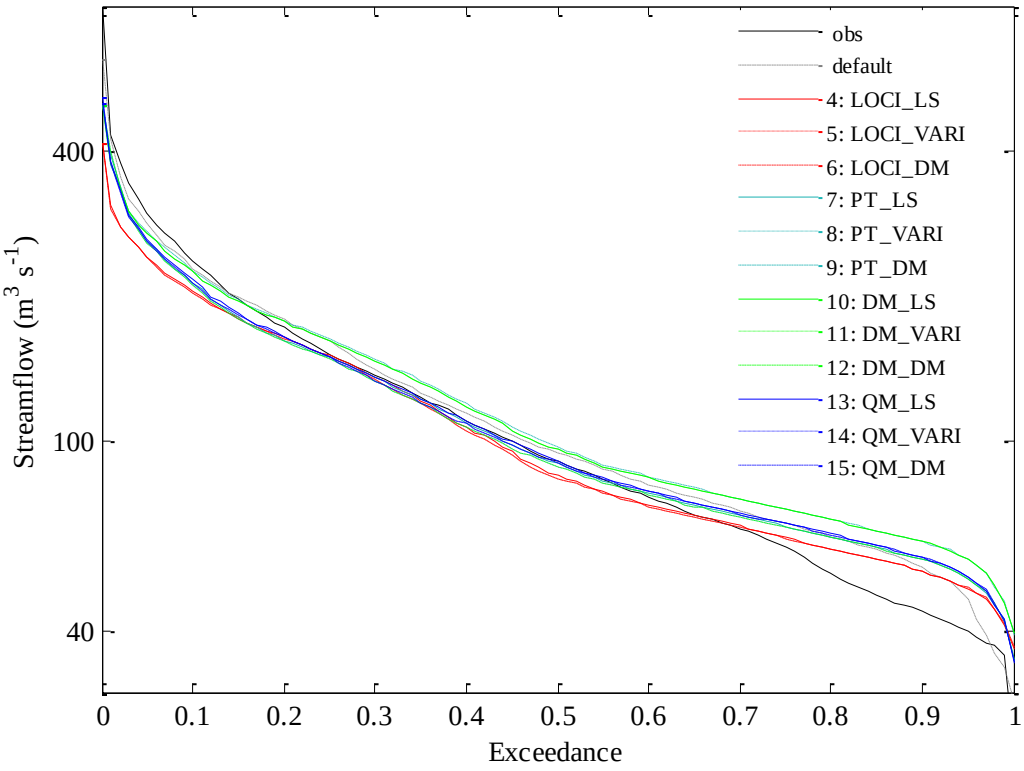

Fig. 7. Exceedance probability curves of observed ("obs") and simulated streamflow driven by observed ("default"), and bias-corrected meteorological data (numbers from 4 to 15; see Table 3 for detailed setup of these simulations).

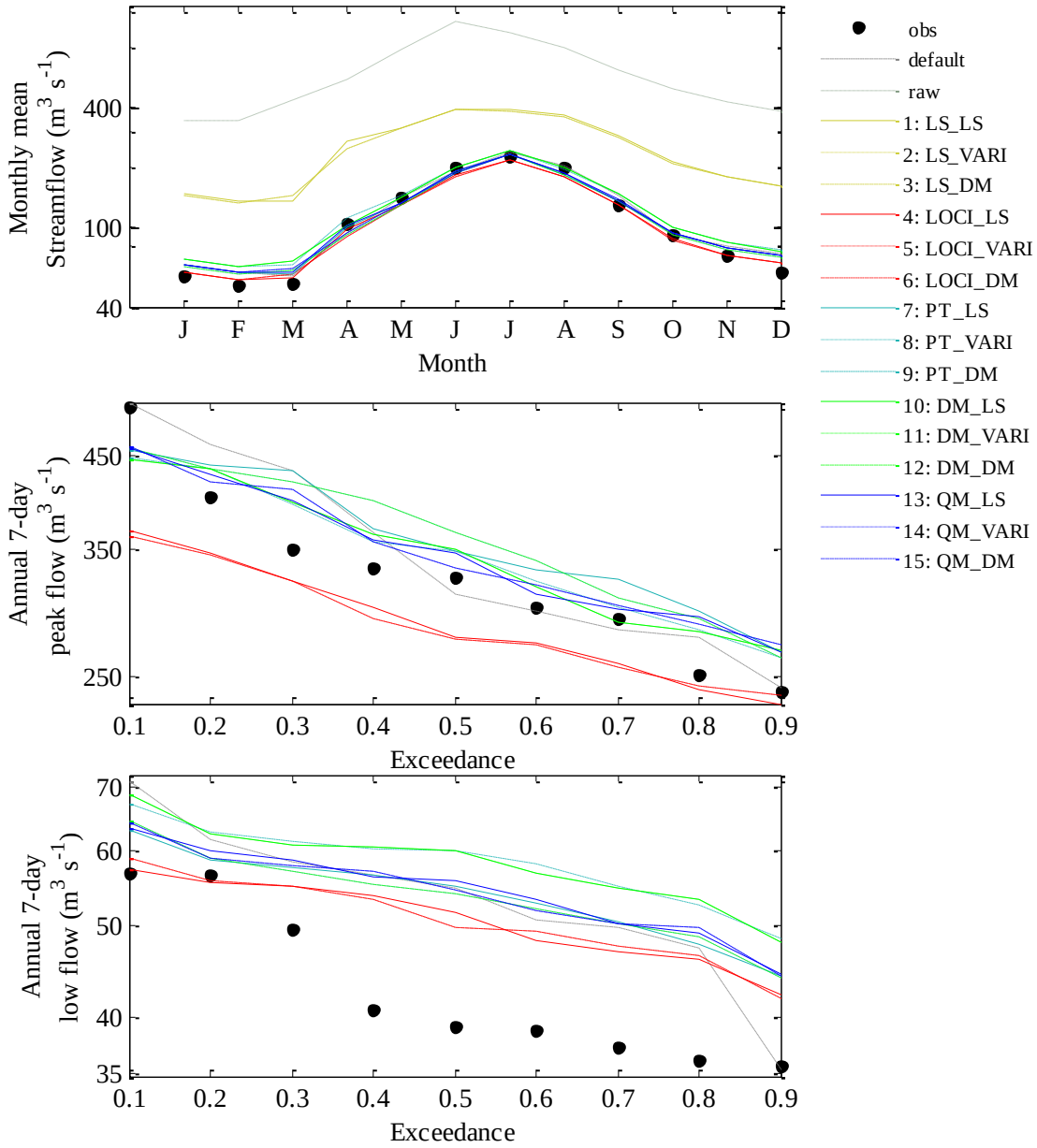

771

772 **Fig. 8.** Monthly mean streamflow (top) and exceedance probability curves of annual 7-day peak
773 flow (middle) and annual 7-day low flow (bottom) during 1986 ~ 2001 in the Kaidu River Basin
774 (obs: observed streamflow; default: simulated with observed meteorological data; raw: simulated
775 with RCM simulated meteorological data; 1~15: simulated with corrected RCM meteorological
776 data listed in Table 3).

777

778